Contemporary Engineering Sciences, Vol. 10, 2017, no. 2, 73 - 84
HIKARI Ltd, www.m-hikari.com
https://doi.org/10.12988/ces.2017.611173

Dynamic Analysis of Centrifugal Separator in Unsteady-State Condition with and without Variable-Frequency Drive

Dario Friso

Department TESAF – Land, Environment, Agriculture and Forestry
Research Unit: Agricultural and Food Engineering
University of Padova, Viale dell'Università 16, I-35020, Legnaro, Padova, Italy

Abstract

The centrifugation process for the separation and/or the clarification of food and chemical liquids, requires complex and expensive machines called centrifugal separator. For example, the insertion of an expensive gear-box between the electric motor and the body of the separator and a longer starting time (about 10 min) are required. In an attempt to solve these two problems, in this work, the use of a modern multi-phase motor supplied by a variable-frequency drive (VFD) and without the gear-box has been considered. About the starting phase and the corresponding unsteady-state condition, a dynamic analysis of the traditional system, in comparison to the proposed one, was conducted. Thus, the starting time for the two cases was compared. The system with variable-frequency drive (VFD) presented a lower time (-16%) compared to the traditional one. This reduction of the starting time was found to be greater if the motor allows a starting phase with overload (-42%). Furthermore, through the equations obtained from the dynamic analysis, the starting time has been correlated with the rated power of the motor. By maintaining the high starting time in about 10 min, the equations give a halving of rated power of motor + VFD overloaded, compared to the traditional system, with a further advantage on the reduction of investment costs.

Keywords: Centrifugal separator, Dynamic analysis, Unsteady-state condition, Asynchronous motor, Variable-frequency drive (VFD), Food engineering

1. Introduction

The centrifugation process for the separation of liquids of different density and/or the clarification of turbid liquids in the food and chemical industry, requires the use of complex and therefore expensive machines [1, 2, 3, 4, 5, 6, 7, 8, 9, 10, 11 and 12].
The reasons for these high costs are due to the high rotational speed to be reached, also over 10,000 RPM. Therefore, the construction and the installation must be very accurate, to avoid dangerous imbalance during rotation [13, 14 and 15]. In addition, an expensive gear-box (multiplier), between the electric motor and the machine parts, must be inserted.

The time required in the starting phase of the centrifugal separator is another aspect that must be considered. In fact, the high inertia of the rotating parts and the high rotation speed would require the use of a very powerful electric motor [16] to make the starting phase rapid.
To avoid over-sizing of the electric motor, a greater acceleration time is accepted. The compromise between the operational requirement and the cost of the motor, has led to accept acceleration times of the order of 10 minutes.

In the present work, a dynamical analysis [17] to correlate the acceleration time with the characteristics of the centrifugal separator, the gear-box and the asynchronous poly-phase electric motor [18] will be made. A second dynamical analysis [19] will be made on a mechanically simpler system, and therefore less expensive, because it will be without the gear-box. To solve the problem of the rotation speed rise between the motor and the centrifugal separator, the multi-phase electric motor will be equipped with a variable-frequency drive (VFD) or simply called inverter [20], able to electro-dynamically increase the rotation speed. The results of the two dynamic analysis will allow to see if a reduction in acceleration times will be possible, in addition to the reduction of investment costs.

2. Dynamical analyses

2.1 Influence of air friction

During the starting phase, the separator is not fed with the liquid to be clarified. Therefore, the internal parts of the separator (Fig. 1), as the bowl and the discs, only undergo the air friction. In this section, we want to check if the air friction can be neglected without compromising the final results of the dynamic analysis. For this purpose and for reasons of simplicity, a constant mechanical power of the electric motor has been supposed (ideal motor).

The corresponding equation of the dynamics of the rotary motion of the centrifugal separator is:

$$I\frac{d\omega_C}{dt} = T_C - T_R = \frac{P_C}{\omega_C} - k\omega_C^2 \tag{1}$$

where: I is the moment of inertia; $d\omega_C /dt$ is the angular acceleration; T_C is the torque from the gear box; T_R is the torque due to air resistance; P_C is the mechanical power, considered constant, from gear box to centrifugal separator; ω_C is the angular velocity of the separator; k is the air drag coefficient.
The solution of the ODE (1) is:

$$t = \frac{I}{6k^{2/3}P_C^{1/3}}\left[\ln\left(\frac{k^{2/3}\omega_C^2 + k^{1/3}\omega_C P_C^{1/3} + P_C^{2/3}}{\left(k^{1/3}\omega_C - P_C^{1/3}\right)^2}\right) - 2\sqrt{3}\arctan\left(\frac{k^{1/3}\omega_C + P_C^{1/3}}{\sqrt{3}P_C^{1/3}}\right)\right] + C \tag{2}$$

The C constant is obtained by initial condition: $\omega_C = 0$ when $t = 0$.

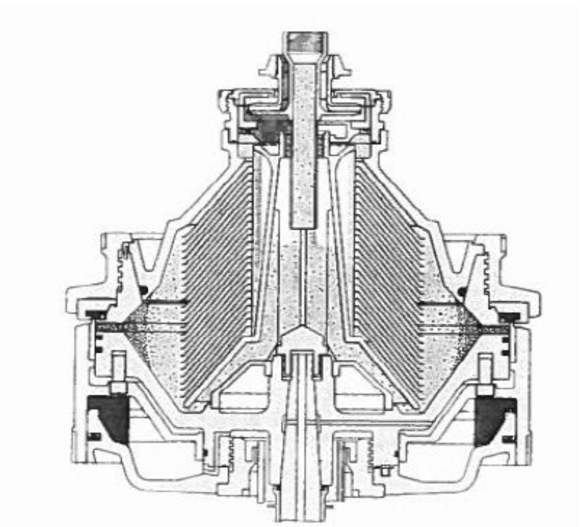

Fig. 1 – Centrifugal separator with discs and bowl

Without drag resistance the eq. (1) becomes:

$$I\frac{d\omega_C}{dt} = \frac{P_C}{\omega_C} \tag{3}$$

And the solution is simply:

$$t = \frac{I \cdot \omega_C^2}{2 \cdot P_C} + C \tag{4}$$

For the same initial condition ($\omega_C = 0$ when $t = 0$), then C=0.
Considering the typical value of centrifugal separator parameters, as shown in table 1, time t furnished by (4) and (2) differs only of the 0.2%. Therefore the next

dynamical analysis in unsteady-state condition [21] during the starting time, about the effective motor without and with variable-frequency drive (VFD), can be conducted neglecting air drag resistance.

Table 1 – Parameters of a typical centrifugal separator

Moment of inertia	I (kgm^2)	32
Motor power	P_M (kW)	20
Gear-box efficiency	η_{GB}	0.94
Power to centr. separator	P_C (kW)	18.8
Air drag coefficient	K (Ns^2)	$3 \cdot 10^{-7}$
Final angular velocity	ω_{CF} (s^{-1})	750

2.2 Centrifugal separator with three-phase asynchronous motor and gear-box without variable-frequency drive (VFD)

This is the traditional system which provides the mechanical feed to separator by using a three-phase asynchronous motor and gear-box. The motor [22], with two poles, has a mechanical power P_M, as in table 1, with delta connection also during starting time. The starting period is scheduled without the liquid to process.
With the European network electric frequency equal to 50 Hz, the synchronous angular speed of the motor is ω_{MS} = 314 s^{-1} and to have a torque T_M>0, a sleep s, as the difference between synchronous speed and operating speed, is necessary. Considering the torque that the separator needs during the steady-state condition to process the liquid, the sleep s is:

$$s = \frac{\omega_{MS} - \omega_{MR}}{\omega_{MS}} = 0.04 \tag{5}$$

Where: ω_{MS} is the synchronous angular speed; ω_{MR} is the rotor angular speed. From the (5) this last is 301 s^{-1}.

For this case, the electro-dynamical equation furnishes the motor torque T_M vs. the sleep s (fig. 2):

$$T_M = \frac{K_1 s}{K_2 + K_3 s^2} \tag{6}$$

Where: K_1, K_2 and K_3 are constant parameters depending from the motor.

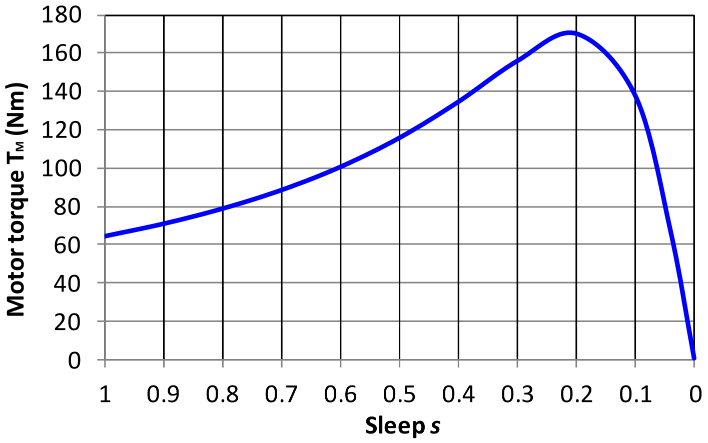

Fig. 2 – Torque T_M vs. sleep s for the three-phase asynchronous motor

By combining (5) and (6), the equation of rotational motion, in unsteady-state condition, is:

$$I\frac{d\omega_{MR}}{dt}=\frac{K_1\left(1-\frac{\omega_{MR}}{\omega_{MS}}\right)}{K_2+K_3\left(1-\frac{\omega_{MR}}{\omega_{MS}}\right)^2} \tag{7}$$

Recalling that the separator angular speed is $\omega_C = \tau\cdot\omega_{MR}$, where τ is the speed ratio and ω_{MR} is the rotor angular speed and that the gear-box efficiency is $\eta_{GB}=\frac{P_C}{P_M}=\frac{T_C}{T_M}\cdot\tau$, the previous (7) becomes:

$$I\frac{d\omega_C}{dt}=T_C=T_M\frac{\eta_{GB}}{\tau}=\frac{K_1\frac{\eta_{GB}}{\tau}\left(1-\frac{\omega_C}{\tau\cdot\omega_{MS}}\right)}{K_2+K_3\left(1-\frac{\omega_C}{\tau\cdot\omega_{MS}}\right)^2} \tag{8}$$

The solution [23] of ODE (8) is:

$$t=\frac{I\tau}{\eta_{GB}}\left[\frac{K_3}{K_1}\left(\omega_C-\frac{\omega_C^2}{2\cdot\tau\cdot\omega_{MS}}\right)-\frac{K_2}{K_1}\tau\cdot\omega_{MS}\ln\left(\left|\omega_C-\tau\cdot\omega_{MS}\right|\right)\right]+C \tag{9}$$

The C constant is obtained by initial condition: $\omega_C = 0$ when $t = 0$.

2.3 Centrifugal separator with three-phase asynchronous motor and variable-frequency drive (VFD) without gear-box

In modern asynchronous motors with variable-frequency drive (VFD) , that is, motors equipped with an electronic system of the power supply frequency adjustment, it is possible to obtain curves of the torque vs. speed characterized by a first portion at a constant torque (power increasing linearly) until the peak value, corresponding to the angular speed ω_{MP}. The second part of the torque-speed curve, instead is characterized by a constant power, and then by a torque decreasing according to a hyperbola. (fig. 3).

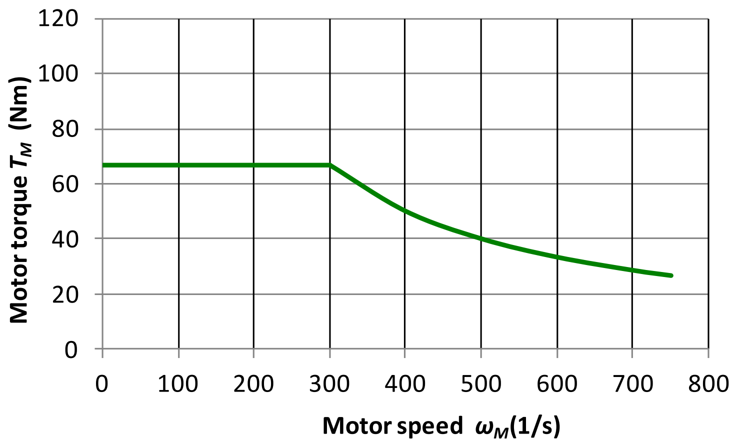

Fig. 3 – Torque T_M vs. motor speed ω_M for the three-phase asynchronous motor with variable-frequency drive (VFD) without overload

With asynchronous two-pole motor, the power supply with a frequency of 50 Hz produces a synchronous angular speed of the motor ω_{MS} = 314 s^{-1}, but the presence of the inverter allows to increase the frequency up to bring the maximum angular speed to about 450-500 s^{-1}. It is a low value for the rotation of the centrifugal separator, but if the electric motor is also built to withstand higher speed, a maximum speed ω_{Mmax} = 750 s^{-1}, corresponding to that request from the separator ω_{CF} (tab.1) can be reached.
The advantage of such a system lies in the elimination of the gear-box, which more than offsets the higher cost of the motor + variable-frequency drive (VFD).
The starting time, corresponding to the first portion of the curve of figure 3, is derived from the simple equation of dynamics:

$$I\frac{d\omega_M}{dt} = T_M \tag{10}$$

Where: ω_M is the angular speed of the motor during the starting time and it is equal to the angular speed of the centrifugal separator ω_C; the torque T_M is constant and equal to: $T_M = P_M / \omega_{MP}$; if ω_{MP} is 301 s^{-1} and P_M is like in the table 1, then T_M is 66.5 Nm. The solution of (10) from 0 to ω_{MP}, is:

$$t_1 = \frac{I}{P_M}\omega_{MP}^2 \tag{11}$$

The second stretch of the torque speed curve corresponds to the time t_2 to accelerate the centrifuge from the peak velocity ω_{MP} = 301 at maximum speed $\omega_{Mmax} = \omega_{CF}$ = 750 s^{-1}. The time t_2 is obtained from the integration of the dynamic equation with constant power P_M, and then with the variable torque $T_M = P_M / \omega_M$:

$$I\frac{d\omega_M}{dt} = \frac{P_M}{\omega_M} \tag{12}$$

$$t_2 = \frac{I}{2P_M}\left(\omega_{M\max}^2 - \omega_{MP}^2\right) \tag{13}$$

During the starting time, in many electrical motors, an increase of current for a short time of the order of some minutes, is possible. This increase of the absorbed current, during the starting time, allows to obtain a torque curve vs. speed, as in figure 4, with an increase of torque up to a peak value $T_{MP} = 1.5 \cdot T_M = 1.5 \cdot 66.5 = 100Nm$ (see eq. (1)), in the first portion of the curve corresponding to the interval t_1. This increase of T_M vs. $\omega_M = \omega_C$ is like a parabola:

$$T_M = a \cdot \omega_M^2 + b \cdot \omega_M + c \tag{14}$$

Where: a, b and c are constants depending of the motor and the variable-frequency drive (VFD) . The (14) is valid for per $0 \le \omega_M \le \omega_{MP}$ = 301 s^{-1}.
Therefore, the equation of the dynamics is:

$$I\frac{d\omega_M}{dt} = a \cdot \omega_M^2 + b \cdot \omega_M + c \tag{15}$$

The solution of the ODE (15), from 0 to ω_{MP}, is:

$$t_1 = \frac{I}{\sqrt{b^2 - 4ac}}\ln\left[\frac{\sqrt{b^2 - 4ac} - \left(b + 2a\omega_{MP}\right)}{\sqrt{b^2 - 4ac} + \left(b + 2a\omega_{MP}\right)}\right] \tag{16}$$

For the next leg of the curve of torque vs. speed (fig. 4), to accelerate the centrifugal separator from the peak speed ω_{MP} = 301 s^{-1} at maximum speed ω_{Mmax} = 750 s^{-1}, the time t_2 is obtained through eq. (13), where: $P_M = P_{MP} = 1.5 \cdot 20 = 30kW$.

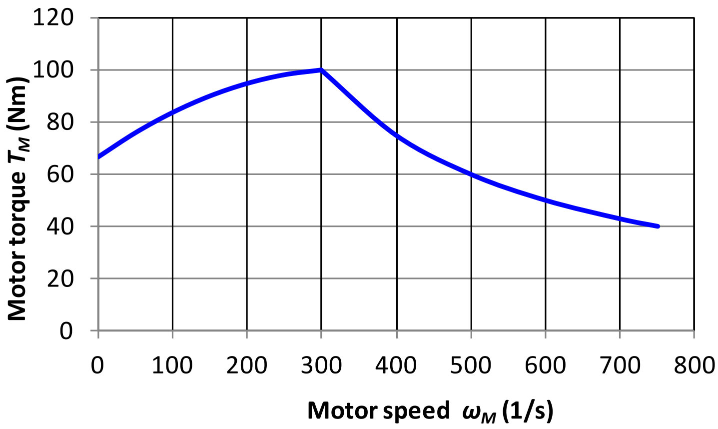

Fig. 4 – Torque T_M vs. motor speed ω_M for the three-phase asynchronous motor with variable-frequency drive (VFD) in overload

3. Results

The specifications of electric motors in comparison, are presented in Table 2. The torque curve vs. speed of standard three-phase asynchronous motor without variable-frequency drive (VFD) is presented in Figure 2, while the curve of the torque vs. speed for the motor with variable-frequency drive (VFD) without overload, is visible in Figure 3. Instead figure 4 shows the torque-speed curve when the motor during the starting phase is overloaded.

The input of the data (Tab. 2) in equations (9), (11), (13) and (16), provides the starting time in the three cases: asynchronous standard motor with gear-box, asynchronous motor with VFD and no overload and motor with VFD and overload.

Figure 5 shows the results obtained. The total starting time of the motor with variable-frequency drive (VFD) is lower than the standard motor with gear-box, of the 16%. More favorable is the result of the motor with VFD and in overload, with a reduction of the starting time equal to 42%.

Finally, equations (13) and (16), obtained from the dynamical analysis in unsteady-state condition for the motor with the VFD in overload, allowed to correlate the starting time with the rated power of the electric motor. Figure 6 shows the starting time vs. the rated power and indicates the maintaining of starting time in about 10 min, as accepted by the industrial community, corresponding to halving of motor power compared to the traditional system, with a further advantage on the reduction of investment costs.

Table 2 - Parameters of the electric motors

Three-phase asynchronous motor with gear-box without VFD	Rated motor power	P_M (kW)	20
	Sleep	s	0.04
	Synchronous angular speed	ω_{MS} (s^{-1})	314
	Rotor angular speed	ω_{MR} (s^{-1})	301
	Constant torque-speed curve	K_1	1662.5
	Constant torque-speed curve	K_2	0.964
	Constant torque-speed curve	K_3	24.94
	Speed ratio (separator/motor)	τ	2.5
	Gear-box efficiency	η_{GB}	0.94
Three-ph. asyn. motor with VFD without gear-box	Rated motor power	P_M (kW)	20
	Peak rotor angular speed	ω_{MP} (s^{-1})	301
	Maximum rotor angular speed	ω_{Mmax} (s^{-1})	750
Three-phase asynchronous motor with VFD overloaded without gear-box	Rated motor power	P_M (kW)	20
	Peak motor power	P_{MP} (kW)	30
	Peak rotor angular speed	ω_{MP} (s^{-1})	301
	Maximum rotor angular speed	ω_{Mmax} (s^{-1})	750
	Constant torque-speed curve	a	-0.000296
	Constant torque-speed curve	b	0.2
	Constant torque-speed curve	c	66.5

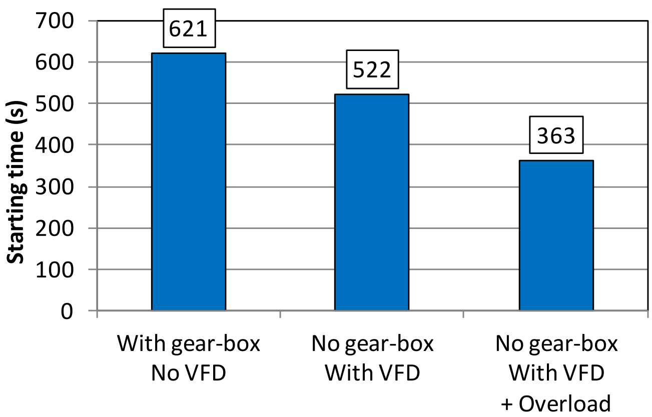

Fig. 5 – Starting time t vs. system

4. Conclusions

The construction and use of centrifugal separators present, respectively, two problems: 1) the insertion of an expensive gear-box between the asynchronous poly-phase electric motor and the body of the separator; 2) a long starting time of the machine.

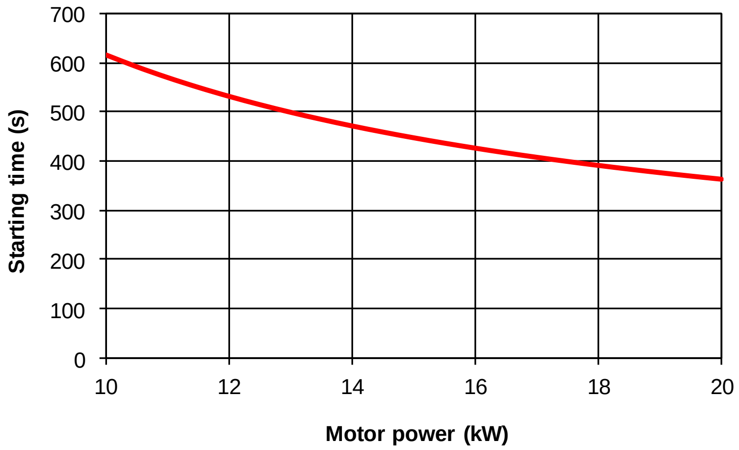

Fig. 6 – Starting time *t* vs. rated power P_M of the motor with variable-frequency drive (VFD) in overload

In an attempt to solve these two problems, in this work the use of a modern multi-phase motor supplied by an variable-frequency drive (VFD) has been considered. That is, a system able to reach the high speeds of rotation required by the separator without the installation of the gear-box.
Moreover, given the starting phase and the corresponding unsteady-state condition, a dynamic analysis of the traditional system, in comparison to the proposed one, was conducted. Thus, the starting time for the two cases was compared. The system with VFD presented a lower time (-16%) compared to the traditional one. This reduction of the starting time was found to be greater if the motor allows a starting phase with overload (-42%).
Finally, through the equations obtained from the dynamic analysis in unsteady-state condition, the starting time has been correlated with the rated power of the electric motor. Therefore, the maintaining of the starting time, accepted by the industrial community and equal to about 10 min, furnishes a halving of rated power of motor + VFD overloaded, compared to the traditional system, with a further advantage on the reduction of investment costs.

References

[1] V. Batalović, Centrifugal separator, the new technical solution, application in mineral processing, *International Journal of Mineral Processing*, **100** (2011), 86–95. https://doi.org/10.1016/j.minpro.2011.05.007

[2] M.E. Afonin, P.N. Belanin, New centrifugal separators for oil cleaning, *Vestnik Masinostroenia*, **12** (1978), 38–42.

[3] Alfa Laval, *The S-Separator, Technical Information for Mineral Oil Treatment*, (2009), www.alfalaval.com

[4] H. Axelsson, B. Madsen, *Centrifuges, Sedimentation*, Alfa Laval separation AB, (2008) Sweden. www.alfalaval.com

[5] B. Benker, A. Wollmann, M. Sievers, Centrifugal flotation as a method for separating oils and fats from wastewater, *Chem. Ing.Tech.*, **74** (2002), 494–500.

[6] M. Colic, W. Morse J.D. Miller, The development and application of centrifugal flotation systems in wastewater treatment, *Int. J. Environ. Pollut*., **30** (2007), 296–312. https://doi.org/10.1504/ijep.2007.014706

[7] S. Fiscor, Separation technology for oil sands, *Engineering and Mining Journal*, **210** (2009), no. 7, 62–63.

[8] K. Gaaseidnes, J. Turbeville, Separation of oil and water in oil spill recovery operations, *Pure Appl. Chem.*, **71** (1999), 95–101. https://doi.org/10.1351/pac199971010095

[9] GEA Westfalia Separator, *Mechanical Separation Technology*, (2009), www.westfalia-separator.com

[10] M.H. Møllekær, B. Madsen, Research results in surprising advances in decanter centrifuges, *Proc. Water and Wastewater International*, **18** (2003), 25–27.

[11] E. Mondt, *Centrifugal Separator of Dispersed Phases*, PhD Theses, University Press, Eindthoven, 2005. alexandria.tue.nl/extra2/200513466.pdf

[12] P.A. Schweitzer, *Handbook of Separation Techniques for Chemical Engineers*, third ed., McGraw-Hill, 1997.

[13] V. I. Dekhanov, N. A. Ratynskaya, Development of high productivity liquid centrifugal separator drives, *Chemical and Petroleum Engineering*, **49** (2013), no. 3–4, 162-166. https://doi.org/10.1007/s10556-013-9719-3

[14] V. I. Dekhanov, V.L. Makhtinger, Variable drive of centrifugal separator, *Chemical and petroleum Engineering*, **23** (1987), no. 1, 3-5. https://doi.org/10.1007/bf01150641

[15] Z. Zhao, Y. Wang, Analysis of the impact on the dish centrifugal separator's drum stress of rotary drum parameters, *Proceedings of International*

Conference on Consumer Electronics, Communications and Networks, (2012), 2402-2404.https://doi.org/10.1109/cecnet.2012.6201769

[16] Colantoni, F. Mazzocchi, F. Cossio, M. Cecchini, R. Bedini and D. Monarca, Comparisons between Battery Chainsaws and Internal Combustion Engine chainsaws: Performance and Safety, *Contemporary Engineering Sciences*, **9** (2016), no. 27,1315-1337. https://doi.org/10.12988/ces.2016.68133

[17] D. Friso, C. Baldoin, Mathematical modeling and experimental assessment of agrochemical drift using a wind tunnel. *Applied Mathematical Sciences*, **9** (2015), no. 110, 5451–5463. https://doi.org/10.12988/ams.2015.56424

[18] Sirio R. S. Cividino, Franco Blanchini, Rosario Lombardo, Daniele Dell'Antonia, Tihana D. Vujinovic, Olga Malev, Rino Gubiani , An Improved Safety Device for Electric Chainsaws, *Contemporary Engineering Sciences*, **8** (2015), no. 27, 1229-1244. http://dx.doi.org/10.12988/ces.2015.56180

[19] D. Friso, H.-P. Haller, M. Zingerle, Mathematical modeling of the dynamics of a shovel with flexible coupling, *Applied Mathematical Sciences*, **9** (2015), no. 110, 5465-5475. http://dx.doi.org/10.12988/ams.2015.56433

[20] Andrey Sheka, Wheeled Mobile Robot Kuzma I, *Contemporary Engineering Sciences*, **7** (2014), no. 18, 895-899. https://doi.org/10.12988/ces.2014.47102

[21] A. Koomsubsiri and D. Sukawat, Solving a Two Dimensional Unsteady-State Flow Problem by Meshless Method, *Applied Mathematical Sciences*, **7** (2013), no. 49, 2421-2428. https://doi.org/10.12988/ams.2013.13219

[22] S.R.S. Cividino, F. Blanchini, R. Lombardo, D. Dell'Antonia, T.D. Vujinovic, O. Malev, R. Gubiani, An improved safety device for electric chainsaws, *Contemporary Engineering Sciences*, **8** (2015), no. 27, 1229-1244. http://dx.doi.org/10.12988/ces.2015.56180

[23] D. Friso, C. Baldoin, F. Pezzi, Mathematical Modeling of the Dynamics of Air Jet Crossing the Canopy of Tree Crops during Pesticide Application, *Applied Mathematical Sciences*, **9** (2015), no. 26, 1281–1296. https://doi.org/10.12988/ams.2015.5145

Received: November 19, 2016; Published: December 30, 2016